

# Uncertainty-Aware Few-Shot Image Classification

Zhizheng Zhang<sup>1\*</sup> Cuiling Lan<sup>2</sup> Wenjun Zeng<sup>2</sup> Zhibo Chen<sup>1</sup> Shih-Fu Chang<sup>3</sup>

<sup>1</sup>University of Science and Technology of China <sup>2</sup>Microsoft Research Asia <sup>3</sup>Columbia University

zhizheng@mail.ustc.edu.cn, {culan, wezeng}@microsoft.com,

chenzhibo@ustc.edu.cn, sc250@columbia.edu

## Abstract

Few-shot image classification aims to learn to recognize new categories from limited labelled data. Recently, metric learning based approaches have been widely investigated which classify a query sample by finding the nearest prototype from the support set based on the feature similarities. For few-shot classification, the calculated similarity of a query-support pair depends on both the query and the support. The network has different confidences/uncertainty on the calculated similarities of the different pairs and there are observation noises on the similarity. Understanding and modeling the uncertainty on the similarity could promote better exploitation of the limited samples in optimization. However, this is still underexplored in few-shot learning. In this work, we propose Uncertainty-Aware Few-Shot (UAFS) image classification by modeling uncertainty of the similarities of query-support pairs and performing uncertainty-aware optimization. Particularly, we design a graph-based model to jointly estimate the uncertainty of similarities between a query and the prototypes in the support set. We optimize the network based on the modeled uncertainty by converting the observed similarity to a probabilistic similarity distribution to be robust to observation noises. Extensive experiments show our proposed method brings significant improvements on top of a strong baseline and achieves the state-of-the-art performance.

## 1 Introduction

The strong capability of deep learning in part relies on a large number of labeled data for training, while humans are more readily able to learn knowledge quickly given a few examples. Few-shot learning (Vinyals et al. 2016; Finn, Abbeel, and Levine 2017; Karlinsky et al. 2019; Dong and Xing 2018; Mishra et al. 2018) strives to a further step to develop deep learning approaches which aim to generalize well to unseen (but related) tasks/classes with just few labeled samples (*i.e.*, requiring/using limited labeled data). Among them, few-shot image classification (Vinyals et al. 2016; Snell, Swersky, and Zemel 2017; Sung et al. 2018; Oreshkin, López, and Lacoste 2018; Finn, Abbeel, and Levine 2017; Nichol, Achiam, and Schulman 2018; Lee et al. 2019) has attracted much attention, which aims to classify data (query samples) of new categories given only a

few labeled samples of these categories as examples (support samples).

For the few-shot image classification, several latest research works reveal that good feature embedding is amenable to deliver favorable classification performance for the similarity-based classification (Chen et al. 2019, 2020; Huang and Tao 2019; Tian et al. 2020). They average the feature embeddings of the support samples of a category to be the prototype of this category. Thus, with each prototype being category-specific, the set of prototypes plays the role of similarity-based classifier, which could identify the class of a query sample by finding the nearest prototype over the support set in the embedding space. During training, for a query sample, the logit vector (classification probability) is obtained through feeding the similarities between the query sample and the prototypes to a SoftMax function. Hence, the representativeness of the learned feature embedding and the reliability of the estimated similarity is vital to the classification performance.

The quality of the output of the network has been investigated and modeled with uncertainty in regression, classification, segmentation, multi-task learning (Kendall, Badrinarayanan, and Cipolla 2015; Kendall and Gal 2017; Chang et al. 2020; Kendall, Gal, and Cipolla 2018) to benefit the optimization. Aleatoric uncertainty identifies the confidence level of the output of the network and it captures the noise inherent in the observations. For few-shot image classification, the network actually has different uncertainties on the calculated similarities of different query-prototype pairs. An observed similarity of a query-prototype pair, being a one time sampling, suffers from observation noise, where the higher of the uncertainty, the less reliable of the estimated similarity. *For each few-shot task during the optimization, the number of experienced query-prototype pairs is limited and thus the side effect of observation noises due to the high uncertainty limits the optimization. Therefore, modeling uncertainty is especially vital for few-shot learning with the limited samples, but still under-explored.*

In this paper, we propose an efficient uncertainty-aware few-shot image classification framework by modeling uncertainty and performing uncertainty-aware optimization. For the similarity-based few-shot image classification, particularly, we model the data-dependent uncertainty of the similarities between a query sample and the  $N$  prototypes

\*This work was done when Zhizheng Zhang was an visiting student at Columbia University.

of the support set through a graph-based model. To be robust to observation noises, for each query-prototype pair, we convert the observed similarity to a distribution (*i.e.*, probabilistic similarity). The similarity-based classification losses are calculated based on the Monte Carlo sampling on the similarity distributions to alleviate the influence of observation noises.

In summary, our contributions lie in the following aspects:

- We are the first to explore and model the uncertainty of the similarity of a query-prototype pair in few-shot image classification, where a better understanding of the limited data is particularly important.
- We design a model to jointly estimate the uncertainty of the similarities between a query image and the prototypes in the support set.
- We perform uncertainty-aware optimization to make the few-shot learning more robust to observation noises.

We conduct comprehensive experiments and demonstrate the effectiveness of our proposed uncertainty-aware few-shot classification method. We conduct all our experiments in the popular inductive (non-transductive) setting, where each query sample is evaluated independently from other query samples. Our scheme achieves the state-of-the-art performance on multiple public datasets. We will release our code and models when the paper is accepted.

## 2 Related Work

### 2.1 Few-shot Image Classification

Few-shot image classification aims to recognize novel (unseen) classes upon limited labeled examples, which requires to generalize the accrued knowledge from base/seen classes to novel (unseen) classes. Representative approaches can be grouped in four categories.

**Classification-based methods** train both a feature extractor and classifiers with meta-learning and learn a new classifier (*e.g.*, linear softmax classifier) for the novel classes during meta-testing (Chen et al. 2019; Ren et al. 2019; Lee et al. 2019). They in general need to update/fine-tune the network given a few-shot testing task.

**Optimization-based methods** exploit more efficient meta-learning optimization strategies for few-shot learning (Finn, Abbeel, and Levine 2017; Grant et al. 2018; Nichol, Achiam, and Schulman 2018; Lee et al. 2019). MAML (Finn, Abbeel, and Levine 2017) is a representative work, which trains models on a variety of learning tasks, such that only a few iterations are needed to achieve rapid adaptation for a new task. It achieves this by updating network parameters with the gradients jointly derived from several tasks.

**Hallucination-based methods** enhance the performance by augmenting data, which alleviates data deficiency by using the generated data. The generators transfer appearance variations (Hariharan and Girshick 2017; Gao et al. 2018) or styles (Antoniou, Storkey, and Edwards 2018) from base classes to novel classes. Wang *et al.* create an augmented training set through a hallucinator/generator which is trained end-to-end along with the classification algorithm (Wang et al. 2018b).

**Metric-based methods** classify an unseen instance to its nearest class based on the similarities with a few labeled examples. They aim to learn to project different instances to a metric space wherein the similarities among instances of the same category are larger than that of instances of different categories. Many approaches follow the meta-learning framework, which trains the model with few-shot tasks sampled in training data. Matching networks (Vinyals et al. 2016) propose to assign an unlabeled data with the label of its nearest labeled data in one-shot learning. Furthermore, the prototypical network (Snell, Swersky, and Zemel 2017) averages the features of several samples of the same category as the prototype of this class and classify unseen data by finding the nearest prototype in the support set. Here, the prototype is taken as the representation of a class and plays a role of the class centroid. Relation networks (Sung et al. 2018) propose an additional relation module as a learnable metric jointly trained with deep feature representations.

Some recent metric-based works reveal that training/pre-training the network with a (fully connected layer) classifier with cosine metric is helpful for learning good feature representations for few-shot tasks (Chen et al. 2019; Tian et al. 2020; Chen et al. 2020). They thus propose strong baselines by training the network with classification supervision over all base classes and further performing meta-learning on sampled categories to simulate the few-shot setting. Chen *et al.* confirmed that the classification-based pre-training can provide extra transferability from base classes to novel classes in the meta-learning stage (Chen et al. 2020).

In this paper, on top of such a strong baseline, we look into an important but still under-explored issue, *i.e.*, modeling and exploiting the inherent uncertainty of the calculated similarities for better optimization.

### 2.2 Uncertainty in Deep Learning

For deep neural network, there are two main types of uncertainty that can be modeled: aleatoric uncertainty, and epistemic uncertainty (Kendall and Gal 2017; Gal 2016; Kendall, Gal, and Cipolla 2018). Epistemic uncertainty captures model-related stochasticity, including parameters choices, architecture, *etc.* Aleatoric uncertainty captures the noise inherent in the observations (Kendall and Gal 2017; Gal 2016; Kendall, Gal, and Cipolla 2018). The aleatoric uncertainty can be further divided into two sub-categories.

Heteroscedastic uncertainty, as a sub-category of aleatoric uncertainty, is *data-dependent*, which depends on the input data of the model, with some noisy inputs or rarely seen inputs potentially having lower confidence on the output/prediction. For per-pixel semantic segmentation and depth regression tasks, input-dependent *heteroscedastic uncertainty* are considered as loss attenuation for better optimization (Kendall and Gal 2017). In contrast, homoscedastic uncertainty is a quantity which is the same for all input data and varies between different tasks. It is thus also described as *task-dependent uncertainty*. It has been adopted in weighting the loss function for multi-task learning (Kendall, Gal, and Cipolla 2018).

For few-shot learning classification, the “hardness” of a few-shot episode is quantified with a metric in (Dhillon et al.

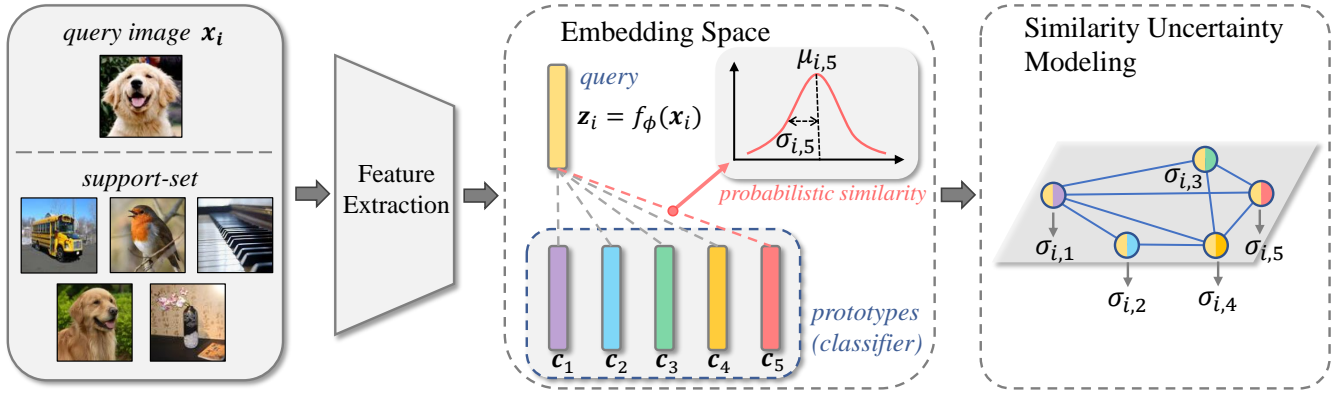


Figure 1: **Pipeline of proposed Uncertainty-Aware Few-Shot (UAFS) image classification.** To alleviate the influence of observation noises on the similarity of a query-prototype pair, rather than a scalar value, we model the similarity between a query feature  $\mathbf{z}_i$  and a prototype feature  $\mathbf{c}_j$  (where  $j = 1, \dots, N$ ) by a distribution, *i.e.*, *probabilistic similarity*, based on graph-based similarity uncertainty estimation. For a query sample  $\mathbf{x}_i$  and  $N$  prototypes in the support set, we take each query-prototype pair as a node and employ a graph-based model to jointly infer the similarity uncertainty  $\sigma_{i,j}$  for each query-prototype pair. The network is optimized with the similarity-based classification losses which exploit the estimated uncertainty (not shown in this figure, please see the subsection around (5)).

2020). However, this metric is only used to evaluate few-shot algorithms rather than improve them in training. In (Wang et al. 2020), a statistical approach is adopted to measure the credibility of predicted pseudo-labels for unlabeled samples in the semi-supervised or transductive few shot learning setting, where the modeled credibility is used for selecting the most trustworthy pseudo-labeled instances to update the classifier. There is still a lack of exploration of the uncertainty for more general inductive few-shot setting, where the network does not use/need testing samples for updating.

In this paper, we model the data-dependent uncertainty of the calculated similarities between a query sample and the prototypes, and leverage it to better optimize the network in the training. To the best of our knowledge, we are the first to explore the uncertainty of pair-similarity in few-shot classification for a more efficient optimization.

### 3 Proposed Uncertainty-aware Few-shot Image Classification

We propose a Uncertainty-Aware Few-Shot (UAFS) image classification framework (see Figure 2). In order to efficiently exploit the limited samples in the episodic training, we model the uncertainty of the estimated similarities between a query and the prototypes to eliminate the side effects of observation noises. Particularly, given a query and the  $N$  prototypes, we use a graph-based network to jointly learn the  $N$  uncertainty values for the similarities of the  $N$  query-prototype pairs. Based on the estimated uncertainty, we represent the similarity as a distribution for each query-prototype pair. Then, we perform Monte Carlo sampling on the distributions of similarities for more accurate loss estimation and optimization.

To be self-included, we first introduce the problem formulation and a strong baseline in Section 3.1. Then, we elaborate our proposed uncertainty-aware few-shot image classi-

fication in Section 3.2.

#### 3.1 Preliminaries and a Strong Baseline

**Problem Formulation.** For few-shot image classification, all the categories/classes of the dataset are divided into base classes  $\mathcal{C}_{base}$  for training and novel classes  $\mathcal{C}_{novel}$  for testing without class overlapping (Snell, Swersky, and Zemel 2017; Chen et al. 2019; Dhillon et al. 2020). In few-shot learning, episodic training is widely used. Each  $N$ -way  $K$ -shot task randomly sampled from base classes is defined as an episode, where the support set  $\mathcal{S}$  includes  $N$  classes with  $K$  samples per class, and the query set  $\mathcal{Q}$  contains the same  $N$  classes with  $M$  samples per class. Our method belongs to the metric-based few-shot learning which performs similarity-based classification based on matching the prototypes in the support set for a given query sample.

Given an image  $\mathbf{x}_i$ , we feed it to a Convolution Neural Network (CNN) to obtain a feature map, and perform global averaging pooling to get a  $D$ -dimensional feature vector  $\mathbf{z}_i = f_\phi(\mathbf{x}_i) \in \mathbb{R}^D$  as the embedding result of  $\mathbf{x}_i$ , where  $f_\phi(\cdot)$  denotes the feature extractor. The prototype of a class indexed by  $k$  is calculated by averaging the feature embeddings of all the samples in the support set of this class as:

$$\mathbf{c}_k = \frac{1}{|S_k|} \sum_{(\mathbf{x}_i, \mathbf{y}_i) \in S_k} f_\phi(\mathbf{x}_i), \quad (1)$$

where  $\mathbf{x}_i$  denotes the sample indexed by  $i$  and  $\mathbf{y}_i$  denotes its label,  $S_k$  denotes the set of samples of the  $k$ -th class in the support set  $\mathcal{S} = \{S_1, \dots, S_N\}$ ,  $|S_k|$  denotes the number of samples in  $S_k$ . Given a query image  $\mathbf{x}$ , the probability of classifying it to the class  $k$  is:

$$p(\mathbf{y}_i = k / \mathbf{x}_i) = \frac{\exp(\tau \cdot s(f_\phi(\mathbf{x}_i), \mathbf{c}_k))}{\sum_{j=1}^N \exp(\tau \cdot s(f_\phi(\mathbf{x}_i), \mathbf{c}_j))}, \quad (2)$$

where the temperature parameter  $\tau$  is a hyper-parameter, and  $N$  is the number of classes in the support set (*i.e.*,  $N$ -way). The  $s(f_\phi(\mathbf{x}_i), \mathbf{c}_k)$  represents the similarity between the given query-sample  $\mathbf{x}_i$  and the prototype  $\mathbf{c}_k$  of the class  $k$ . For metric-based few-shot image classification, the  $N$  prototypes of  $N$  classes in the support set construct the similarity-based classifier.

**Baseline.** Many works (Vinyals et al. 2016; Snell, Swersky, and Zemel 2017; Bauer et al. 2017; Chen et al. 2019; Li et al. 2019; Chen et al. 2020) reveal that the core of metric-based few-shot learning is to learn a good feature embedding function  $f_\phi(\cdot)$  from base classes  $\mathcal{C}_{base}$  which could generalize well on unseen classes. We follow the latest work (Chen et al. 2020) which simply leverage both the classification-based pre-training and the meta-learning training to build the strong baseline with the two stages:

*Stage-1: Classification-based pre-training.* We employ a Fully-Connected (FC) layer as the classifier with cosine similarity metric over all base classes. We train the feature extractor  $f_\phi(\cdot)$  (backbone network) and the classifier in an end-to-end manner using a standard cross-entropy loss.

*Stage-2: Meta-learning.* For each episode/task, we sample  $N$ -way  $K$ -shot from base classes for training, which can be understood as a simulation of few-shot test process. In each task,  $N \times K$  images and  $N \times M$  images are sampled to constitute the support set and the query set, respectively. We adopt the cross-entropy loss formulated by  $\mathcal{L} = -\sum_{i=1}^{N \times M} \mathbf{y}_i \cdot \log(p(\mathbf{y}_i/\mathbf{x}_i))$ , where  $p(\mathbf{y}_i/\mathbf{x}_i)$  is calculated in Eq. (2) with  $s(\cdot, \cdot)$  instantiated by cosine similarity.

### 3.2 Uncertainty-aware Few-shot Learning

For a given model, it has different uncertainties regarding its outputs for different input data and there will be observation noises for an instantiated output. For similarity-based few-shot image classification, the class of a query (instance) is determined based on its similarity with the prototypes in the support set. The model has uncertainty on the estimated similarities for the query-prototypes pairs. The small number of samples in each few-shot episode exacerbate the side effect of observation noises. To address this, we model the data-dependent uncertainty of similarities and leverage it for better optimizing the network.

**Probabilistic Similarity Representation.** To model the uncertainty of similarity of a query-prototype pair, we convert the similarity representation of this query-prototype pair from a deterministic value to a probabilistic representation (*i.e.*, a distribution). In this way, the similarity uncertainty can be modeled by the parameters of the distribution.

Given a query sample  $\mathbf{x}_i$  (with its feature  $\mathbf{z}_i = f_\phi(\mathbf{x}_i)$  in the latent space) and a prototype  $\mathbf{c}_j$  obtained by Eq. (1), instead of being a deterministic value, we model their similarity as a probability distribution. Similar to many other works (Kendall and Gal 2017; Gal 2016), we simply model the distribution of the similarity between this query and the prototype  $\mathbf{c}_j$  by a Gaussian distribution with mean  $\mu_{ij}$  and variance  $\sigma_{ij}^2$ :

$$p(\mathbf{s}_{ij}|\mathbf{z}_i, \mathcal{C}) = \mathcal{N}(\mathbf{s}_{ij}; \mu_{ij}, \sigma_{ij}^2 I), \quad (3)$$

where  $\mathcal{C} = \{\mathbf{c}_1, \dots, \mathbf{c}_N\}$  denotes the  $N$  prototypes in the support set. We estimate the mean of the similarity by their inner product, *i.e.*,  $\mu_{ij} = \langle \mathbf{z}_i, \mathbf{c}_j \rangle$ , which denotes the most likely value of the similarity between  $\mathbf{z}_i$  and  $\mathbf{c}_j$ . The variance  $\sigma_{ij}^2$  denotes **the uncertainty of this pairwise similarity**. We estimate it by a graph neural network with trainable parameters, which will be elaborated in the subsection ‘‘Similarity Uncertainty Modeling’’. With the similarity of a query-support pair being a distribution rather than a deterministic value, we enable a differentiable instantiated representation of the probabilistic similarity  $\mathbf{s}_{ij}$  by re-parameterizing it as:

$$\mathbf{s}_{ij,t} = \mu_{ij} + \sigma_{ij} \epsilon_t, \quad \epsilon_t \in \mathcal{N}(0, 1). \quad (4)$$

**Uncertainty-aware Optimization.** To reduce the side effect of observation noises in the optimization of a few shot episode, we calculate the loss based on the distributions of similarities (*i.e.*, probabilistic similarities). However, the analytic solution of integrating over these distributions for the optimization of loss function is difficult. We thus approximate the objective by Monte Carlo integration. We achieve this by using Monte Carlo sampling on the  $N$  similarity distributions. Particularly, for a given query image  $\mathbf{x}_i$  and  $N$  prototypes  $\mathbf{c}_j, j = 1, \dots, N$  which form  $N$  similarity pairs, we repeat  $T$  random sampling over the similarity distributions for each query-prototype pair  $\mathbf{s}_{ij}$  (see (4) with  $t = 1, \dots, T$ ) to obtain statistical results. Therefore, for a given query image  $\mathbf{x}_i$  with groundtruth label  $\mathbf{y}_i = k$ , we obtain its corresponding classification loss as:

$$\mathcal{L}(\mathbf{x}_i, \mathbf{y}_i = k) = -\log\left(\frac{1}{T} \sum_{t=1}^T (e^{\mathbf{s}_{ik,t}} / \sum_{j=1}^N e^{\mathbf{s}_{ij,t}})\right). \quad (5)$$

**Similarity Uncertainty Modeling.** We propose a Graph Neural Network (GCN) based model to jointly estimate the similarity uncertainties (denoted by the variances of the similarity distributions) for  $N$  query-prototype pairs.

To estimate the uncertainty  $\sigma_{ij}$  of the similarity between the query image  $\mathbf{x}_i$  and the prototype  $\mathbf{c}_j$  of the class  $j$ , one solution is to use the information of this pair to infer  $\sigma_{ij}$ . However, similarity-based  $N$  class classification is a joint determination process, where the query is compared with all the  $N$  prototypes and the class of the prototype with the highest similarity value is taken as the predicted class. The joint determination nature inspires us to estimate uncertainty  $\sigma_{ij}$  for each pair after taking a global glance of the  $N$  pairs with  $j = 1, \dots, N$ . Therefore, we design a graph-based model as the similarity uncertainty estimator to jointly infer all the  $\sigma_{ij}$  for a given query  $\mathbf{x}_i$  and  $N$  prototypes  $\mathbf{c}_j$ . This enables the exploration of global scope information for the current task to jointly estimate the similarity uncertainties. Unlike the previous work (Garcia and Bruna 2018), which adopts graph-based model to propagate information from labeled samples to unlabeled ones thus delivers a transductive solution, we use graph-based model to achieve the joint estimation of uncertainty of  $N$  query-prototype pairs for a given query (non-transductive), where the uncertainty is used to better optimize the network. Our graph-based model is discarded in testing. The GCN in (Garcia and Bruna 2018) is a part of their network and is needed during testing.

The feature of a query image  $\mathbf{x}_i$  is denoted as  $\mathbf{z}_i = f_\phi(\mathbf{x}_i) \in \mathbb{R}^D$  and the prototypes of its support set are denoted by  $\mathbf{c}_j \in \mathbb{R}^D, j = 1, \dots, N$ . We use the group-wise relations/similarities between the query and the  $j^{\text{th}}$  prototype feature to represent the information of this query-prototype pair. Specifically, we split both  $\mathbf{z}_i$  and  $\mathbf{c}_j$  into  $L$  groups along their channel dimensions to have  $\{z_i^l | l = 1, \dots, L\}$  and  $\{c_j^l | l = 1, \dots, L\}$ , where  $L \leq D$ . We calculate the cosine similarity of the  $l^{\text{th}}$  group as  $r_{ij}^l = \frac{z_i^l c_j^{lT}}{\|z_i^l\| \|c_j^l\|}$ , and stack them to be a relation feature vector  $\mathbf{v}_{ij} = [r_{ij}^1, \dots, r_{ij}^L] \in \mathbb{R}^L$ . In this simple way, we make use of the similarities with respect to different semantics of feature (in different channel groups) to infer the uncertainty of similarity.

Given a query and  $N$  prototypes, we build a graph of  $N$  nodes, with the  $j^{\text{th}}$  node denoted by the information of the query and the  $j^{\text{th}}$  prototype. The output of the node is the predicted uncertainty of the similarity of this query-prototype pair. The  $N$  nodes in the graph are represented by a matrix  $V_i = (\mathbf{v}_{i1}; \dots; \mathbf{v}_{iN}) \in \mathbb{R}^{N \times L}$ . We use graph convolutional network (GCN) to learn the similarity uncertainty for each node. Similar to (Shi et al. 2019; Wang et al. 2018a; Wang and Gupta 2018), the edge from the  $j^{\text{th}}$  node to the  $j'^{\text{th}}$  node is modeled by their affinity in the embedded space, which is formulated as:

$$E_i(j, j') = \varphi_1(\mathbf{v}_{ij})\varphi_2(\mathbf{v}_{ij'})^T, \quad (6)$$

where  $\varphi_1$  and  $\varphi_2$  denote two embedding functions implemented by FC layers. All edges constitute an adjacent matrix denoted by  $E_i \in \mathbb{R}^{N \times N}$ . We normalize each row of  $E_i$  with SoftMax function so that all the edge values connected to a target node is 1, yielding a numerically-stable message passing through the modeled graph. Similar to (Wang et al. 2018a), we denote the normalized adjacent matrix by  $G_i$  and update the nodes through GCN as:

$$V_i' = V_i + Y_i W_y, \quad \text{where } Y_i = G_i V_i W_v, \quad (7)$$

$W_v \in \mathbb{R}^{L \times L}$  and  $W_y \in \mathbb{R}^{L \times L}$  are two learnable transformation matrices.  $W_v$  is implemented by a  $1 \times 1$  convolutional layer.  $W_y$  is implemented by two stacked blocks. Each block consists of a  $1 \times 1$  convolution layer, followed by a Batch Normalization (BN) layer and an LeakyReLU activation layer. We thus infer the similarity uncertainty vector  $\mathbf{u}_i = [\sigma_{i1}, \dots, \sigma_{iN}] \in \mathbb{R}^N$  for the  $N$  pairs from the updated graph nodes, which can be formulated as:

$$\mathbf{u}_i = \alpha(\text{BN}(V_i' W_{u1})) W_{u2}, \quad (8)$$

where the  $j^{\text{th}}$ -dimension of  $\mathbf{u}_i$  is the aforementioned  $\sigma_{ij}$ , denoting the similarity uncertainty for the query  $\mathbf{x}_i$  and the  $j^{\text{th}}$  prototype.  $W_{u1} \in \mathbb{R}^{L \times L}$  and  $W_{u2} \in \mathbb{R}^{L \times 1}$  are transformation matrices both implemented by a  $1 \times 1$  convolutional layer. ‘‘BN’’ refers to the Batch Normalization layer and  $\alpha(\cdot)$  refers to the LeakyReLU activation function.

Discussion: For similarity-based few-shot classification, the class estimation of a query image is influenced by not only the query itself but also the prototypes in the support set. Therefore, different from the uncertainty modeling in depth regression, segmentation (Kendall and Gal 2017)

which model the uncertainty based on the sample itself, we model the uncertainty of similarity based on *both the query sample and the prototypes*. We further conduct extensive experiments to compare the effectiveness of modeling feature uncertainty (query itself) vs. similarity uncertainty (query and prototypes) for few-shot image classification in our experiments. Moreover, in our ablation study, we also compare our graph-based modeling with non-graph-based modeling (*i.e.* Conv-based), which infers the uncertainty of a query-prototype pair based on the pair itself.

Besides, our proposed similarity uncertainty estimator is scalable to the number of classes for classification, which allow us to optimize it during different training stages as introduced in the next subsection.

**Joint Training.** Similar to the baseline configuration described in Section 3.1, we train the entire network in two stages: *classification-based pre-training* and *meta-learning*.

In the *classification-based pre-training* stage, we perform classification over all classes of  $\mathcal{C}_{base}$ . The learned FC layer coefficients of the classifier play a role of class centers, which can be considered as the prototypes in similarity-based classification. The classification scores are obtained by calculating the cosine similarity between the instance feature and those class centers (prototypes). From this perspective, the *classification* in the two stages are unified.

In the *meta-learning* stage, we sample  $N$ -way  $K$ -shot episodic tasks from base classes and perform episodic training. Actually, our proposed similarity uncertainty modeling and optimization is applicable to both stages. In the *classification-based pre-training* stage, the FC coefficients can be considered as the prototypes and the number of input nodes in GCN is the total number of classes in  $\mathcal{C}_{base}$ . In the *meta-learning* stage, the number of input nodes in GCN is  $N$ . The parameters in GCN are shared in the two stages. We fine-tune the backbone and the similarity uncertainty estimator in the *meta training* stage.

Note that we do not introduce any complexity increase in the testing where the uncertainty estimator is discarded.

## 4 Experiments

### 4.1 Dataset and Implementation

**Datasets:** For few-shot image classification, we conduct experiments on four public benchmark datasets: mini-ImageNet (Vinyals et al. 2016), tiered-ImageNet (Ren et al. 2018), CIFAR-FS (Bertinetto et al. 2018), and FC100 (Oreshkin, López, and Lacoste 2018) (See our Supplementary for more detailed introduction). Both mini-ImageNet and tiered-ImageNet are built upon ImageNet (Deng et al. 2009) and we use the commonly used  $84 \times 84$  spatial resolution. CIFAR-FS and FC100 are built on CIFAR-100 (Krizhevsky, Hinton et al. 2009) and  $32 \times 32$  spatial resolution is used.

**Networks and Training:** Following recent common practices in this field (Oreshkin, López, and Lacoste 2018; Lee et al. 2019), we adopt a wider ResNet-12 with more channels as the backbone in our work unless claimed otherwise. We build our strong baseline (see Section 3.1) by following (Chen et al. 2020) with two-stage training. For *classification-based pre-training* stage, we train 120

Table 1: Comparison on applying the proposed similarity uncertainty modeling and optimization in different training stages. “Stage1” refers to the *classification-based pre-training* stage while “Stage2” refers to the *meta-learning* stage as described in the manuscript. “no” denotes the corresponding training stage is not used. “w U” denotes that we apply the proposed similarity uncertainty modeling and optimization in the corresponding training stage while the “w/o U” denotes we do not apply it.

Model	Stage1	Stage2	mini-ImageNet		tiered-ImageNet		CIFAR-FS		FC-100	
			1-shot	5-shot	1-shot	5-shot	1-shot	5-shot	1-shot	5-shot
1	w/o U	no	59.28 ± 0.81	78.26 ± 0.60	67.02 ± 0.84	83.56 ± 0.61	71.95 ± 0.81	84.21 ± 0.58	39.42 ± 0.77	54.12 ± 0.79
2	w U	no	61.53 ± 0.83	78.83 ± 0.60	68.77 ± 0.82	83.92 ± 0.42	73.81 ± 0.78	84.54 ± 0.63	41.76 ± 0.52	56.63 ± 0.24
3	w/o U	w/o U	63.10 ± 0.85	79.44 ± 0.65	67.72 ± 0.80	83.61 ± 0.62	72.36 ± 0.67	84.43 ± 0.50	40.23 ± 0.22	56.16 ± 0.56
4	w U	w/o U	63.16 ± 0.66	79.56 ± 0.67	68.92 ± 0.77	83.96 ± 0.56	73.10 ± 0.70	84.68 ± 0.48	40.34 ± 0.59	56.24 ± 0.55
5	w/o U	w U	62.57 ± 0.33	79.35 ± 0.49	69.11 ± 0.83	84.12 ± 0.55	72.51 ± 0.68	84.46 ± 0.49	39.49 ± 0.33	53.24 ± 0.24
6	w U	w U	64.22 ± 0.67	79.99 ± 0.49	69.13 ± 0.84	84.33 ± 0.59	74.08 ± 0.72	85.92 ± 0.42	41.99 ± 0.58	57.43 ± 0.38

Table 2: Comparison on different uncertainty modelling methods. “SampleU” denotes that we estimate the uncertainty of a *query sample* while “SimiU” denotes that we estimate the uncertainty of the *similarity between a query and its prototype*. Besides, we compare different designs of the uncertainty estimator (U-Estimator), including using CNNs (“Conv-based”) to process each sample or each query-prototype pair independently, using GCNs (“Graph-based”) to process the  $N$  query-prototype pairs jointly. “B” denotes the abbreviation of “Meta-Base”.

Methods	U-Estimator	mini-ImageNet		CIFAR-FS	
		1-shot	5-shot	1-shot	5-shot
Meta-Base	-	63.10 ± 0.85	79.44 ± 0.65	72.36 ± 0.67	84.43 ± 0.50
B+ SampleU	Conv-based	63.25 ± 0.81	79.39 ± 0.63	72.11 ± 0.80	84.26 ± 0.52
B+ SimiU	Conv-based	63.31 ± 0.68	79.63 ± 0.46	73.22 ± 0.75	84.40 ± 0.69
B+ SimiU	Graph-based	64.22 ± 0.67	79.99 ± 0.49	74.08 ± 0.72	85.92 ± 0.42

epochs with the batch size of 512 for tiered-ImageNet and 100 epochs with the batch size of 128 for the other three datasets. For *meta-learning* stage, we uniformly sample 4 episodes/tasks per iteration for mini-ImageNet and tiered-ImageNet, and 16 episodes per iteration for CIFAR-FS and FC100. We sample 15 query samples per class (*i.e.*,  $Q = 15$ ) within each episode in training. We adopt the SGD optimizer with the initial learning rate of 0.1 and the weight decay of  $5.e-4$ . For all our models, the classification temperature  $\tau$  in (2) is a trainable parameter which is initialized with 10. We perform data augmentation, including horizontal flip, random crop, and color jitter during training. For the parameter  $L$ , we found the performance is very similar when it is set within the range of 16 to 64 and we set it to 32.

**Evaluation:** We do all experiments in the inductive (non-transductive) setting (*i.e.*, each query sample is evaluated independently from other query samples). We create each few-shot episode by uniformly sampling 5 classes (*i.e.*  $N=5$ ) from the test set and further uniformly sampling support and query samples for each sampled class accordingly. Consistent with other works, we report the mean accuracy and the standard deviation with a 95% confidence interval over 1000 randomly sampled few-shot episodes. Besides, we do not perform fine-tuning using the data on the novel classes (*i.e.*, support set) in testing to make the system simple/easy to use.

## 4.2 Ablation Study

**Effectiveness of Proposed UAFS.** Table 1 shows the ablation study on the effectiveness of the proposed similar-

ity uncertainty modeling and optimization. Model 3 corresponds to our strong baseline *Meta-Base* (see Table 3) with two-stage training. Model 6 corresponds to our final scheme *Meta-UAFS* with the proposed similarity uncertainty modeling and optimization (UMO).

We have the following observations. **1)** Based on the strong baseline, our proposed *Meta-UAFS* (Model-6) improves *Meta-Base* (Model-3) by 1.12%, 1.41%, 1.72% and 1.76% in 1-shot classification on four datasets respectively, which demonstrates the effectiveness of our UMO. **2)** Model-3 obviously outperforms Model-1, demonstrating the effectiveness of two-stage training as a strong baseline. **3)** Model-2 with UMO obviously outperforms Model-1 but Model-4 only slightly outperforms Model-3. The higher the performance, the more difficult it is to obtain gain. On top of the strong baseline, the UMO is not helpful for Stage-1 which does not suffer from limited training data as Stage-2. **4)** Applying the UMO only for the *meta-learning* stage does not always bring improvements. Applying the UMO on both stages brings significant improvements. In the *meta-learning* stage for model-5, the backbone is pre-trained but the similarity uncertainty estimator is trained from scratch, resulting in the difficulty in optimizing the estimator with limited data. Since our proposed graph-based similarity uncertainty estimator is scalable to the number of classes, this allows us to use the estimator with shared parameters in *classification-based pre-training* stage, which effectively reduces the difficulty of optimization (playing a pre-training role for the similarity uncertainty estimator). Therefore, our final proposed model (Model-6) delivers the best results. Note that in *meta-learning* state, the number of training samples in a task is small and the side-effect of observation noise is more harmful. Observation 3) and 4) show that a well designed UMO (with pre-training) is very helpful for meta-learning where the number of training samples in a task is small.

**Similarity Uncertainty Estimator Designs.** For a query and the  $N$  prototypes, we can independently estimate the uncertainty value for each query-prototype pair. However, since the class of the query is actually jointly determined by comparing it with the  $N$  prototypes. Thus, we propose to use a GCN to jointly estimate the uncertainty values. Table 2 shows that our *Graph-based* similarity uncertainty estimator (last row) obviously outperforms the *Conv-based* similarity uncertainty estimator (the penultimate row) which uses  $1 \times 1$  convolutional layers to independently infer the uncertainty

Table 3: Accuracy (%) comparison for 5-way few-shot classification of our schemes, our baselines and the state-of-the-arts on four benchmark datasets. For the backbone network, “ $l_1$ - $l_2$ - $l_3$ - $l_4$ ” denotes a 4-layer convolutional network with the number of convolutional filters in each layer as  $l_1, l_2, l_3, l_4$ , respectively. *classification-based pre-training* stage. “Meta-Base” and “Meta-UAFS” refer to the strong baseline model and our final UAFS model, which are both trained with two stages (the second stage: *meta-learning* stage). The superscript  $\dagger$  refers to that the model is trained on the combination of training and validation sets while others only use the training set. Note that for fair comparisons, all the presented results are from inductive (non-transductive) setting. Bold numbers denotes the best performance while numbers with underlines denotes the second best performance.

Methods	Backbone	mini-ImageNet		tiered-ImageNet		CIFAR-FS		FC-100	
		1-shot	5-shot	1-shot	5-shot	1-shot	5-shot	1-shot	5-shot
MatchingNet (Vinyals et al. 2016)	64-64-64-64	46.6	60.0	-	-	-	-	-	-
MAML (Finn, Abbeel, and Levine 2017)	32-32-32-32	48.70 ± 1.84	63.11 ± 0.92	51.67 ± 1.81	70.30 ± 1.75	-	-	-	-
ProtoNet <sup>†</sup> (Snell, Swersky, and Zemel 2017)	64-64-64-64	49.42 ± 0.78	68.20 ± 0.66	53.31 ± 0.89	72.69 ± 0.74	-	-	-	-
RelationNet (Sung et al. 2018)	64-96-128-256	50.44 ± 0.82	65.32 ± 0.70	54.48 ± 0.93	71.32 ± 0.78	-	-	-	-
TADAM (Oreshkin, López, and Lacoste 2018)	ResNet-12	58.50 ± 0.30	76.70 ± 0.30	-	-	-	-	40.10 ± 0.40	56.10 ± 0.40
LEO <sup>†</sup> (Rusu et al. 2019)	WRN-28-10	61.76 ± 0.08	77.59 ± 0.10	66.33 ± 0.05	81.44 ± 0.09	-	-	-	-
TapNet (Yoon, Seo, and Moon 2019)	ResNet-12	61.65 ± 0.15	76.36 ± 0.10	63.08 ± 0.15	80.26 ± 0.12	-	-	-	-
Shot-free (Ravichandran, Bhotika, and Soatto 2019)	ResNet-12	59.04 ± 0.43	77.64 ± 0.39	66.87 ± 0.43	82.64 ± 0.39	69.20 ± 0.40	84.70 ± 0.40	-	-
MetaOptNet (Lee et al. 2019)	ResNet-12	62.64 ± 0.61	78.63 ± 0.46	65.99 ± 0.72	81.56 ± 0.53	72.00 ± 0.70	84.20 ± 0.50	41.10 ± 0.60	55.50 ± 0.60
CAN (Hou et al. 2019)	ResNet-12	63.85 ± 0.48	79.44 ± 0.34	<b>69.89 ± 0.51</b>	84.23 ± 0.37	-	-	-	-
Baseline2020 (Dhillon et al. 2020)	WRN-28-10	56.17 ± 0.64	73.31 ± 0.53	67.45 ± 0.70	82.88 ± 0.53	70.26 ± 0.70	83.82 ± 0.49	36.82 ± 0.51	49.72 ± 0.55
MetaBaseline (Chen et al. 2020) <sup>1</sup>	ResNet-12	63.17 ± 0.23	79.26 ± 0.17	68.62 ± 0.27	83.29 ± 0.18	-	-	-	-
Meta-Base	ResNet-12	63.10 ± 0.85	79.44 ± 0.65	67.72 ± 0.80	83.61 ± 0.62	72.36 ± 0.67	84.43 ± 0.50	40.23 ± 0.22	56.16 ± 0.56
Meta-UAFS	ResNet-12	<b>64.22 ± 0.67</b>	<b>79.99 ± 0.49</b>	<u>69.13 ± 0.84</u>	<b>84.33 ± 0.59</b>	<b>74.08 ± 0.72</b>	<b>85.92 ± 0.42</b>	<b>41.99 ± 0.58</b>	<b>57.43 ± 0.38</b>

for each query-prototype pair.

**Sample Uncertainty vs. Pair Similarity Uncertainty.** Table 2 shows that the scheme *B+SimiU* with Graph-based uncertainty estimator which models the *uncertainty of the query-prototype similarity* is more effective than the scheme *B+SampleU* which models the *uncertainty of a sample*. That is because in the few shot classification, for a given query, its estimated class depends on both the query and the  $N$  prototypes. Therefore, we model the uncertainty of the similarity between the query and the prototypes.

### 4.3 Comparison with State-of-the-arts

In Table 3, we compare our proposed *Meta-UAFS* with the state-of-the-art approaches. Note that our design of baseline network *Meta-Base* is the same as MetaBaseline<sup>1</sup> (Chen et al. 2020) and they have the similar performance. In comparison with *Meta-Base* (Chen et al. 2020), our *Meta-UAFS* achieves significant improvement of 1.12%, 1.41%, 1.72%, and 1.76% in 1-shot accuracy on mini-ImageNet, tiered-ImageNet, CIFAR-FS, and FC00, respectively for 1-shot classification. Our *Meta-UAFS* achieves the state-of-the-art performance. CAN (Hou et al. 2019) introduces cross attention module to highlight the target object regions, making the extracted feature more discriminative. Our uncertainty modeling and optimization which reduces the side effects of observation noises is complementary to their attention design and incorporating their attention design into our framework would lead to superior performance.

### 4.4 Visualization of Learned Uncertainty

Our exploration of uncertainty could reduce the side effect of observation noises on the similarity during optimization. We visualize the learned uncertainty of many randomly selected query-prototype tasks and find they are consistent with human intuition. Figure 2 shows two examples. Given

<sup>1</sup>In their test code, rather than using the more commonly used number of testing episodes, *i.e.*, 1000, they use 8000. In contrast, we report *Meta-Base* using 1000.

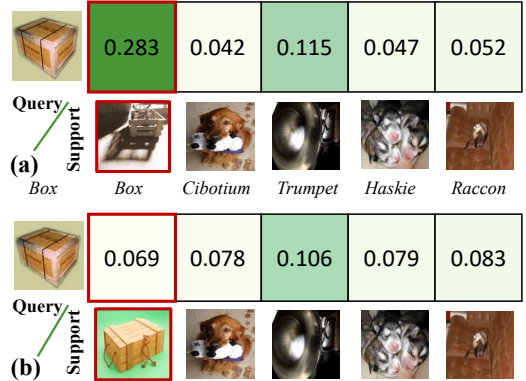


Figure 2: Visualization of learned uncertainty values for two examples.

a fixed query sample of class “Box”, four negative support samples (last four columns) and a positive support sample, when compare (a) and (b), we find the positive pair in (b) has less visual ambiguity than that in (a). Consistently, our learned uncertainty value of 0.069 in (b) is much lower than that (0.283) in (a).

## 5 Conclusion

In this paper, we propose an Uncertainty-Aware Few-Shot image classification approach where data-dependent uncertainty modeling is introduced to alleviate the side effect of observation noise. Particularly, we convert the similarity between a query sample and a prototype from a deterministic value to a probabilistic representation (using a distribution) and optimize the networks by exploiting the similarity uncertainty. We design a graph-based uncertainty estimator to jointly estimate the similarity uncertainty of the query-support pairs for a given query sample. Extensive experiments demonstrate the effectiveness of our proposed method and our scheme achieves state-of-the-arts performance on all the four benchmark datasets.

## Ethics Statement

We are the first to introduce aleatoric uncertainty modeling into few-shot learning. Specifically, we model data-dependent uncertainty for the similarity of query-support pairs in few-shot image classification. The broader impact of our work lies in the following aspects:

**For research community**, we point out the importance of uncertainty exploration in deep learning with limited labeled data (few shot learning) and our solution bring improvement for few-shot image classification. This is overlooked in previous works in this domain. Despite the main focus of our this work is on the modeling of data-dependent uncertainty, we believe it will inspire more studies on uncertainty exploration in the field of few-shot learning. It is exciting to see more extensions to other few-shot tasks, *e.g.* few-shot object detection, few-shot scene segmentation.

**For industry/society**, besides the improvements on few-shot image classification accuracy, this work makes contributions to developing a risk-controlled few-shot recognition system. In many scenarios, we not only expect a higher performance of our system but also want to make sure the risks of using this system can be controlled when facing complex especially health-related application scenarios. Therefore, we would expect the model to reject the results by itself or push it to human decision if it is not confident enough. Intuitively, the output with low confidence is more likely to be given by the models trained with very limited data. Thus, it becomes critical for us to address this problem.

## References

- Antoniou, A.; Storkey, A.; and Edwards, H. 2018. Data augmentation generative adversarial networks. *ICLR*.
- Bauer, M.; Rojas-Carulla, M.; Świątkowski, J. B.; Schölkopf, B.; and Turner, R. E. 2017. Discriminative k-shot learning using probabilistic models. *arXiv preprint arXiv:1706.00326*.
- Bertinetto, L.; Henriques, J. F.; Torr, P. H.; and Vedaldi, A. 2018. Meta-learning with differentiable closed-form solvers. *arXiv preprint arXiv:1805.08136*.
- Chang, J.; Lan, Z.; Cheng, C.; and Wei, Y. 2020. Data Uncertainty Learning in Face Recognition. *CVPR*.
- Chen, W.-Y.; Liu, Y.-C.; Kira, Z.; Wang, Y.-C. F.; and Huang, J.-B. 2019. A closer look at few-shot classification. *ICLR*.
- Chen, Y.; Wang, X.; Liu, Z.; Xu, H.; and Darrell, T. 2020. A new meta-baseline for few-shot learning. *arXiv preprint arXiv:2003.04390*.
- Deng, J.; Dong, W.; Socher, R.; Li, L.-J.; Li, K.; and Fei-Fei, L. 2009. Imagenet: A large-scale hierarchical image database. In *CVPR*, 248–255.
- Dhillon, G. S.; Chaudhari, P.; Ravichandran, A.; and Soatto, S. 2020. A baseline for few-shot image classification. *ICLR*.
- Dong, N.; and Xing, E. 2018. Few-Shot Semantic Segmentation with Prototype Learning. In *BMVC*, volume 3.
- Finn, C.; Abbeel, P.; and Levine, S. 2017. Model-agnostic meta-learning for fast adaptation of deep networks. In *ICML*, 1126–1135. JMLR. org.
- Gal, Y. 2016. *Uncertainty in deep learning*. Ph.D. thesis, University of Cambridge.
- Gao, H.; Shou, Z.; Zareian, A.; Zhang, H.; and Chang, S.-F. 2018. Low-shot learning via covariance-preserving adversarial augmentation networks. In *NeurIPS*, 975–985.
- Garcia, V.; and Bruna, J. 2018. Few-shot learning with graph neural networks. In *ICLR*.
- Grant, E.; Finn, C.; Levine, S.; Darrell, T.; and Griffiths, T. 2018. Recasting gradient-based meta-learning as hierarchical bayes. *arXiv preprint arXiv:1801.08930*.
- Hariharan, B.; and Girshick, R. 2017. Low-shot visual recognition by shrinking and hallucinating features. In *ICCV*, 3018–3027.
- Hou, R.; Chang, H.; Bingpeng, M.; Shan, S.; and Chen, X. 2019. Cross attention network for few-shot classification. In *NeurIPS*, 4003–4014.
- Huang, S.; and Tao, D. 2019. All you need is a good representation: A multi-level and classifier-centric representation for few-shot learning. *arXiv preprint arXiv:1911.12476*.
- Karlinisky, L.; Shtok, J.; Harary, S.; Schwartz, E.; Aides, A.; Feris, R.; Giryas, R.; and Bronstein, A. M. 2019. RepMet: Representative-based metric learning for classification and few-shot object detection. In *CVPR*, 5197–5206.
- Kendall, A.; Badrinarayanan, V.; and Cipolla, R. 2015. Bayesian segnet: Model uncertainty in deep convolutional encoder-decoder architectures for scene understanding. *arXiv preprint arXiv:1511.02680*.
- Kendall, A.; and Gal, Y. 2017. What uncertainties do we need in bayesian deep learning for computer vision? In *NeurIPS*, 5574–5584.
- Kendall, A.; Gal, Y.; and Cipolla, R. 2018. Multi-task learning using uncertainty to weigh losses for scene geometry and semantics. In *CVPR*, 7482–7491.
- Krizhevsky, A.; Hinton, G.; et al. 2009. Learning multiple layers of features from tiny images.
- Lee, K.; Maji, S.; Ravichandran, A.; and Soatto, S. 2019. Meta-learning with differentiable convex optimization. In *CVPR*, 10657–10665.
- Li, H.; Eigen, D.; Dodge, S.; Zeiler, M.; and Wang, X. 2019. Finding task-relevant features for few-shot learning by category traversal. In *CVPR*, 1–10.
- Mishra, A.; Verma, V. K.; Reddy, M. S. K.; Arulkumar, S.; Rai, P.; and Mittal, A. 2018. A generative approach to zero-shot and few-shot action recognition. In *WACV*, 372–380.
- Nichol, A.; Achiam, J.; and Schulman, J. 2018. On first-order meta-learning algorithms. *arXiv preprint arXiv:1803.02999*.
- Oreshkin, B.; López, P. R.; and Lacoste, A. 2018. Tadam: Task dependent adaptive metric for improved few-shot learning. In *NeurIPS*, 721–731.
- Ravichandran, A.; Bhotika, R.; and Soatto, S. 2019. Few-shot Learning with Embedded Class Models and Shot-Free Meta Training. In *ICCV*, 331–339.
- Ren, M.; Liao, R.; Fetaya, E.; and Zemel, R. 2019. Incremental few-shot learning with attention attractor networks. In *NIPS*, 5275–5285.
- Ren, M.; Triantafillou, E.; Ravi, S.; Snell, J.; Swersky, K.; Tenenbaum, J. B.; Larochelle, H.; and Zemel, R. S. 2018. Meta-learning for semi-supervised few-shot classification. *arXiv preprint arXiv:1803.00676*.

- Rusu, A. A.; Rao, D.; Sygnowski, J.; Vinyals, O.; Pascanu, R.; Osindero, S.; and Hadsell, R. 2019. Meta-learning with latent embedding optimization. *ICLR* .
- Shi, L.; Zhang, Y.; Cheng, J.; and Lu, H. 2019. Two-stream adaptive graph convolutional networks for skeleton-based action recognition. In *CVPR*, 12026–12035.
- Snell, J.; Swersky, K.; and Zemel, R. 2017. Prototypical networks for few-shot learning. In *NeurIPS*, 4077–4087.
- Sung, F.; Yang, Y.; Zhang, L.; Xiang, T.; Torr, P. H.; and Hospedales, T. M. 2018. Learning to compare: Relation network for few-shot learning. In *CVPR*, 1199–1208.
- Tian, Y.; Wang, Y.; Krishnan, D.; Tenenbaum, J. B.; and Isola, P. 2020. Rethinking Few-Shot Image Classification: a Good Embedding Is All You Need? *arXiv preprint arXiv:2003.11539* .
- Vinyals, O.; Blundell, C.; Lillicrap, T.; Wierstra, D.; et al. 2016. Matching networks for one shot learning. In *NeurIPS*, 3630–3638.
- Wang, X.; Girshick, R.; Gupta, A.; and He, K. 2018a. Non-local neural networks. In *CVPR*, 7794–7803.
- Wang, X.; and Gupta, A. 2018. Videos as space-time region graphs. In *ECCV*, 399–417.
- Wang, Y.; Xu, C.; Liu, C.; Zhang, L.; and Fu, Y. 2020. Instance Credibility Inference for Few-Shot Learning. *CVPR* .
- Wang, Y.-X.; Girshick, R.; Hebert, M.; and Hariharan, B. 2018b. Low-shot learning from imaginary data. In *CVPR*, 7278–7286.
- Yoon, S. W.; Seo, J.; and Moon, J. 2019. Tapnet: Neural network augmented with task-adaptive projection for few-shot learning. *arXiv preprint arXiv:1905.06549* .